Time-resolved transport between resonantly coupled Landau levels in semiconductor superlattices

F. Claro
Facultad de Física, Pontificia Universidad Católica, Casilla 306, Santiago 22, Chile

J. F. Weisz
Grupo de Física de Materiales, Instituto de Desarrollo Tecnológico para la Industria Química, Guemes 3450, 3000 Santa Fe, Argentina

W. Müller* and K. v. Klitzing
Max-Planck-Institut für Festkörperforschung, Heisenbergstraße 1, D-70569 Stuttgart, Germany

H. T. Grahn† and K. Ploog
Paul-Drude-Institut für Festkörperelektronik, Hausvogteiplatz 5-7, D-10117 Berlin, Germany
(Received 14 August 1995)

Resonant tunneling between Landau levels has been investigated by the time-of-flight technique. The peak photocurrent displays clear resonances due to resonant Landau level tunneling, when the applied electric field is increased. The experimental results are compared with a model calculation that allows scattering-mediated hopping between different Stark as well as Landau levels. Good agreement is obtained if magnetic-field-induced quenching of the scattering rate is incorporated in the model.

I. INTRODUCTION

Resonant tunneling between Landau levels (LL's) has been investigated in semiconductor heterostructures, e.g., in single and double barrier structures as well as superlattices (SL's). All experiments so far have been performed by recording the time-averaged current or conductivity as a function of the applied voltage. The resonances appear as extrema in the I-V characteristics, conductance, or second derivative of the I-V trace.[1–4]

In this paper we report on experiments using time-resolved photocurrent in the picosecond to nanosecond time regime to investigate resonant coupling of Landau levels. Due to the rather long transport times through a superlattice structure in comparison with a single or double barrier structure, it was possible to directly observe the resonant coupling of Landau levels. Furthermore, the experimental results are supported by model calculations, which reproduce the general features of the voltage dependence of the drift velocity rather well.

II. EXPERIMENT

We have investigated a GaAs-AlAs superlattice with 11.3-nm GaAs wells, 1.7-nm AlAs, and 50 periods. The SL and two significantly larger wells on each side of the SL are forming the intrinsic region of a p^+-i-n^+ diode. The p^+ and n^+ regions consist of highly doped $Al_{0.5}Ga_{0.5}As$ layers. The sample has been grown by molecular-beam epitaxy on a (001)-oriented n^+-GaAs substrate and processed into mesas of 120 μm diameter with Ohmic contacts of Cr/Au on the top and AuGe/Ni on the substrate side. The top contact pad has a diameter of 70 μm and therefore covers only 25% of the mesa area in order to ensure that carriers can be generated in the SL via illumination. Under a reverse bias voltage V_A the applied electric field F_A in the SL is given by $F_A=(V_{\rm BI}-V_A)/W$, where $V_{\rm BI}=1.52$ V is the built-in voltage and W is the width of the intrinsic region. In reverse bias no carriers are injected via the contacts.

Time-dependent photocurrent measurements are employed to study the vertical transport in this SL as a function of the applied electric field and magentic field at temperatures of 10 K and below. The principles and experimental details of this time-of-flight (TOF) technique are given in Refs. 4 and 5. Since the maximum of the photocurrent transient is directly proportional to the drift velocity of the generated electrons,[4,5] the TOF measurements represent a powerful tool to study the tunneling dynamics of electrons in these samples. Typical values for the experimentally observed peak photocurrents are 10–100 μA, keeping the total charge Q_0 of the generated electrons below -0.4 pC to avoid space-charge buildup and field inhomogeneities.

III. RESULTS

A. Experiment

The average drift velocity is obtained by measuring the photoexcited current and the photogenerated charge Q_0, which is the integral of the photocurrent over the whole time range. Within a Gaussian transport model, the peak photocurrent is proportional to the drift velocity,[6] i.e.,

$$v_d=\frac{I_{\max}}{Q_0}W, \tag{1}$$

where W denotes the drift distance, which corresponds to the intrinsic width of the p^+-i-n^+ structure. In Fig. 1 the measured drift velocity is shown for a 11.3-nm–1.7-nm GaAs-AlAs superlattice at 0 (a) and 7 (b) T. The typical behavior at vanishing magnetic field consists of an Ohmic regime, where

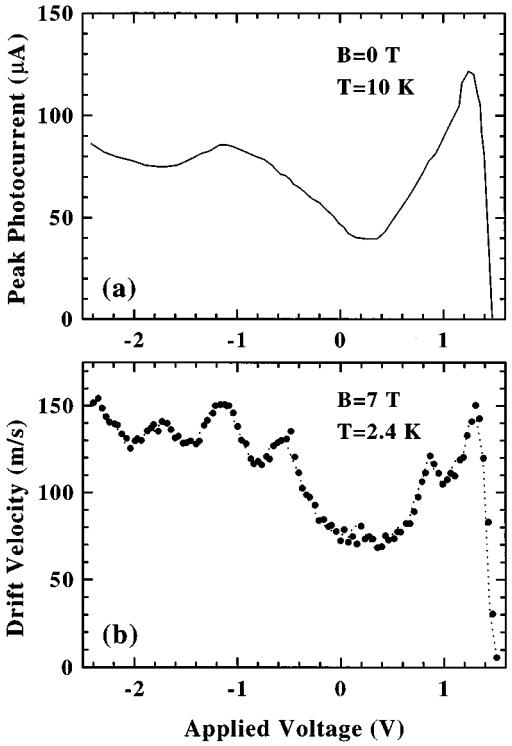

FIG. 1. (a) Peak photocurrent vs applied voltage for a 11.3-nm–1.7-nm GaAs-AlAs superlattice at zero magnetic field recorded at 10 K. (b) Drift velocity vs applied voltage for the same sample for a perpendicular magnetic field of 7 T at 2.4 K.

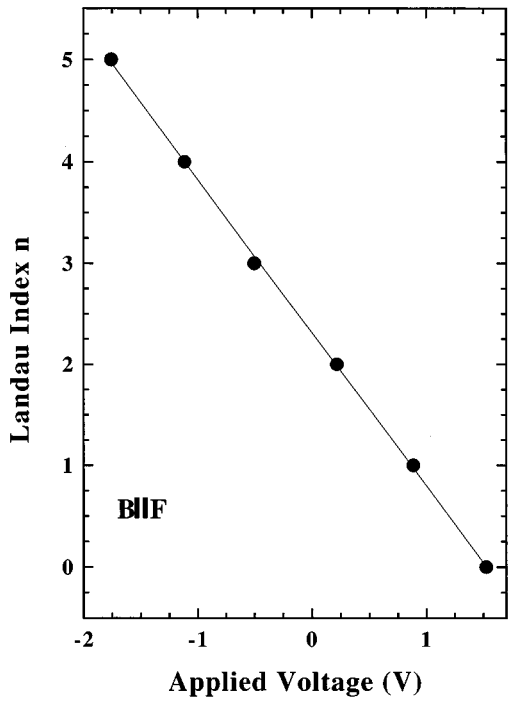

FIG. 2. Maxima of the drift velocity vs applied voltage for the experimental data in Fig. 1(b). The solid line is a linear regression fit to the data points with a slope of $-1.513\ \mathrm{V}^{-1}$, which corresponds to an energy of 12 meV.

the drift velocity is proportional to the effective electric field (between 1.5 and 1.3 V), followed by a maximum and a subsequent decrease of the drift velocitiy. The regime beyond the maximum corresponds to the negative differential velocity regime, which also exists in bulk GaAs, but at much lower field strengths and with much larger peak velocities. After a minimum at 0.25 V, the drift velocity begins to increase again because of two mechanisms. The first one is the nonresonant tunneling background, the second one is the existence of tunneling resonances of different origin. The maximum at -1 V is attributed to tunneling between the lowest electronic subbands with the emission of an longitudinal-optical phonon. At even larger electric fields (lower voltages) resonant tunneling between the first and second electronic subbands is observed (not shown here, cf., e.g., Ref. 5).

The drift velocity recorded in a perpendicular magnetic field of 7 T, however, shows a very different behavior [cf. Fig. 1(b)]. Additional resonances are observed, which can be related to resonant tunneling between Landau levels. In Fig. 2 the resonance peaks are plotted in multiples of the magnetic energy $\hbar\omega_c = \hbar eB/m^*$, where m^* denotes the effective mass. The slope of the straight line corresponds to an energy of 12 meV, in excellent agreement with the cyclotron energy of 12.1 meV at 7 T using the bulk effective mass of GaAs ($m^* = 0.067m$). Although resonant Landau-level tunneling is only possible between Landau levels of the same index, this selection rule is violated by scattering due to phonons and/or lateral inhomogeneities such as interface roughness. We therefore assign the additional structures in the drift velocity to resonant Landau-level tunneling between the lowest LL in one well and a higher LL in the adjacent well. This interpretation will be supported by a model calculation of the transport properties of such a superlattice in a perpendicular electric and magnetic field.

In the following we will focus on the low-field regime. In Fig. 3 the peak drift velocity (a) and corresponding electric-field strength $F_{\max}$ (b) are plotted versus the magnetic field strength between 0 and 7 T. Both quantities decrease with increasing magnetic field strength. This effect can be understood by comparing the results of the one-dimensional model of miniband transport by Ignatov *et al.*[7] with the numerical results of the three-dimensional model by Gerhardts.[8] However, the investigated superlattice has a rather negligible miniband width and the described models are not really applicable. The quantitative behavior, i.e., the rather linear dependence of the maximum drift velocity and the more quadratic dependence of $F_{\max}$, will therefore also be addressed in the next section.

B. Model calculations

The motion of a photoexcited pulse of charge is studied in a GaAs/AlAs superlattice with the parameters given above. The average velocity of the motion of the diffusing charges is calculated theoretically from the velocity picked up by the moving charges and from coherent quantum motion up to a scattering time of the order of a picosecond.

Longitudinal electric and magnetic fields are applied to the superlattice. In the absence of scattering, e.g., due to disorder or phonons, a longitudinal magnetic field would have no effect whatsoever on the motion of charges along the axis of the superlattice. However, the experiment clearly shows resonances due to the presence of Landau levels such

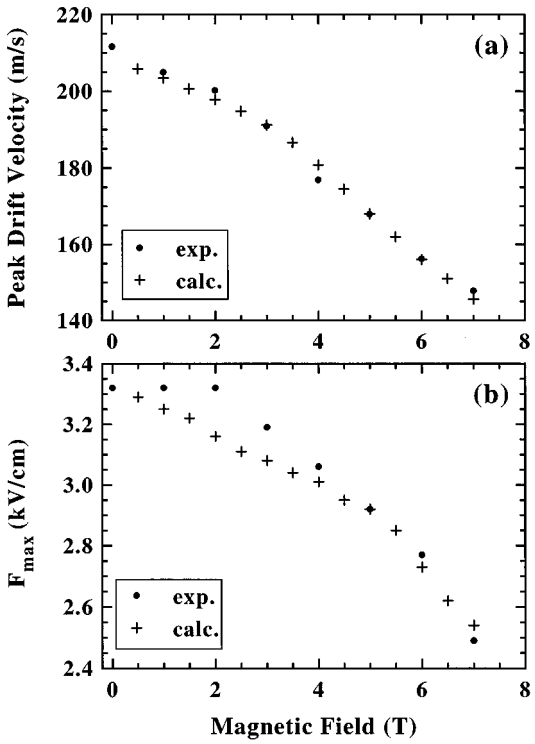

FIG. 3. Peak drift velocity (a) and corresponding electric-field strength $F_{\max}$ (b) vs magnetic field in the 11.3-nm–1.7-nm GaAs-AlAs superlattice at 2.4 K. The dots refer to the experimental results, the crosses to the calculated results.

that the separation of the Stark levels, or some simple fraction thereof, is equal to the separation $\hbar\omega_c$ of the Landau levels. Such resonances are only expected if the levels exhibit a finite width.

The velocity of the pulse, which is of order 150 ms^{-1}, indicates a traversal of the superlattice within a few nanoseconds, while the expected scattering time τ for the carriers is of the order of a picosecond. Undoubtedly one must assume a diffusive process for the charge motion, but up to the scattering time the motion may be assumed to be determined by quantum coherence. The width of the levels Γ is related to the scattering time through $\Gamma=\hbar/\tau$. Thus, if $\Gamma=1$ meV, then $\tau=0.66$ ps.

The experimental data show first a region of rising velocity with increasing electric field (Ohmic region), followed by a maximum and subsequent decrease due to Wannier-Stark localization. It is expected that the decrease will not begin until the separation of the Wannier-Stark levels is larger than their width. Therefore, the position of the peak should roughly be given by the criterion $eaF_c=\Gamma$, where a denotes the superlattice period and F_c the critical field, which leads to a localization of the Wannier-Stark states. This criterion has also been given by Plessen *et. al.*[9]

The time evolution equations valid up to approximately the scattering time are

$$i\hbar\frac{dc_{n,p}}{dt}=E_{n,p}c_{n,p}-\sum_{m,q}\lambda_{n,m}\frac{\Gamma^2}{\Gamma^2+(E_{n,p}-E_{m,q})^2}c_{m,q}, \tag{2}$$

with

$$E_{n,p}=peFa+(n+\tfrac{1}{2})\hbar\omega_c. \tag{3}$$

Here n denotes the Landau-level index, p is the SL site, F is the electric field, and the set $c_{n,p}$ are the expansion coefficients of the wave function in terms of isolated well eigenstates. This set of equations is appropriate for a single miniband with hopping in one dimension only (tight-binding model). The sum over the index q on the right-hand side of Eq. (2) is over nearest neighbors, while the sum over m is over an unrestricted number of Landau levels. For the hopping coefficient $\lambda_{n,m}$ we take the form

$$\lambda_{n,m}=\lambda_F\delta_{n,m}+\lambda_B(1-\delta_{n,m}), \tag{4}$$

where λ_F measures the hopping amplitude between levels with the same Landau index, while λ_B is the amplitude for hopping, when the conservation of Landau index is violated.

Given an initial distribution $c_{n,p}(0)$ the solutions of Eq. (2) characterize the time evolution of the pulse as it propagates through the sample. Its average position at time t is

$$\langle z\rangle=\sum_{n,p}pc^*_{n,p}c_{n,p}a. \tag{5}$$

Differentiating this quantity with respect to time and using Eq. (2) and the symmetry property $\lambda_{n,m}=\lambda_{m,n}$, we get for the velocity of propagation in a large sample the expression

$$v=-\frac{2a}{\hbar}\sum_{m,n}\tilde{\lambda}_{m,n}\mathrm{Im}\left(\sum_p c^*_{m,p}c_{n,p-1}\right), \tag{6}$$

where

$$\tilde{\lambda}_{m,n}=\lambda_{m,n}\frac{\Gamma^2}{\Gamma^2+[eFa+(m-n)\hbar\omega_c]^2}. \tag{7}$$

Analytical solutions are easy to obtain for the case when there is only a longitudinal electric field, e.g., when $B=0$. The first sum in Eq. (6) has then a single term and the velocity and its time derivative become

$$v=-\frac{2\lambda(F)a}{\hbar}\mathrm{Im}\left(\sum_p c^*_pc_{p-1}\right) \tag{8}$$

$$\frac{dv}{dt}=\frac{2\lambda(F)ea^2F}{\hbar^2}\mathrm{Re}\left(\sum_p c^*_pc_{p-1}\right), \tag{9}$$

where

$$\lambda(F)=\lambda_F\frac{\Gamma^2}{\Gamma^2+(eFa)^2}. \tag{10}$$

Here we have suppressed the magnetic index. Both equations involve the quantity

$$A(t)=\sum_p c^*_pc_{p-1}, \tag{11}$$

which, as follows from Eq. (2), obeys the equation of motion,

$$i\hbar\frac{dA}{dt}=-eFaA, \tag{12}$$

This is a first-order differential equation with the solution

$$A(t)=A(0)\exp\left(\frac{ieFat}{\hbar}\right), \tag{13}$$

where $A(0)$ is the value at $t=0$. Using this solution in Eqs. (8) and (9), the dynamics is that of a harmonic oscillator of period $\hbar/eFa$, the well-known Bloch period. Combining Eqs. (8) and (13) we get

$$v=\frac{2\lambda(F)aA(0)}{\hbar}\sin\left(\frac{eFat}{\hbar}\right). \tag{14}$$

If we start with a nonzero amplitude at a single site only, then $A(0)=0$ and $v=0$ at all times. This result was obtained earlier in a many-band treatment by Bouchard and Luban.[10] The pulse will then spread with time, but not move at all in position. The same is true if the initial state is an eigenstate of the Hamiltonian. The eigenfunctions of Eq. (2) of Wannier-Stark energy $qeFa$ are the Bessel functions $c_p=J_{p-q}\{[2\lambda(F)/eFa]\}$.[11] Using these solutions and the summation properties of Bessel functions in Eq. (11) yields $A(0)=0$, and once again the velocity is zero at all times. To obtain an effective motion of the carriers one must place finite values of the amplitudes initially on at least two consecutive sites.

In order to compare the results of this theory with experiment, we consider the average velocity $\bar{v}=[x(t)-x(0)]/t$ rather than the instantaneous velocity given by Eq. (14). Integrating the latter,

$$\bar{v}=\frac{4A(0)}{e\tau}\frac{\lambda(F)}{F}\sin^2\left(\frac{eFa\tau}{2\hbar}\right), \tag{15}$$

where the time t has been replaced by the collision time τ. For values of τ small compared to the period of Bloch oscillations one obtains

$$\bar{v}=\frac{2A(0)a^2e\tau}{\hbar^2}\lambda(F)F. \tag{16}$$

Thus, from Eq. (10) we see that for small fields the velocity grows linearly with the electric field, while at large fields it decreases as $1/F$. In between, a maximum $\overline{v_m}=a\tau A(0)\Gamma\lambda_F/\hbar^2$ is reached.

The above analytic results hold when no magnetic field is present. We have obtained results for the case with magnetic field by numerical integration of Eq. (2). In Fig. 3 the results for the maximum field and peak drift velocity using this approach are included as crosses. The agreement between the calculated and the experimental values is quite good. The data were fitted using the parameter values $\lambda_F=0.2$ meV and $\Gamma=6.0$ meV at $B=0$ T. At finite magnetic fields we varied Γ linearly down to the value $\Gamma=3.9$ meV at $B=7$ T. While λ_F was kept fixed, λ_B was raised linearly from a value of 0 at zero magnetic field to $\lambda_B=0.08$ meV at $B=7$ T. Up to $n=8$ Landau levels were included. Increasing this number did not lead to any significant changes in the results. As a time step we used $\delta t=0.00125\tau$ and iterated Eq. (2) up to a total time of 0.4τ. Initially we set all amplitudes to zero except at three consecutive sites, where they were given the values $\beta, \sqrt{1-2\beta^2}$, and β. In the results shown we used the value $\beta=0.025$, so that the electron is initially well localized around a single site. In practice the displacement of the pulse is small on the time scale of the calculations, so that the boundary conditions at sites 1 and 50 are not a critical factor. One may take these edge amplitudes as zero. All amplitudes were normalized over the whole superlattice so that the current entering from the left equals the current flowing to the right.

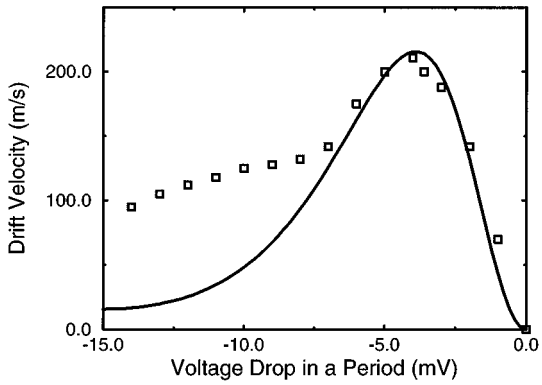

FIG. 4. Drift velocity vs electric field (or applied voltage) in the absence of a perpendicular magnetic field for the 11.3-nm–1.7-nm GaAs-AlAs superlattice at 2.4 K. The squares denote the experimental data, the solid line the calculated drift velocity.

Results as a function of applied bias are shown as solid lines in Figs. 4 and 5 for $B=0$ T and 7 T, respectively. The squares denote the experimental data. In Fig. 4 the parameters $\lambda_F=0.25$ meV and $\Gamma=5.5$ meV were used, while for Fig. 5 we used $\lambda_F=0.22$ meV, $\Gamma=4.0$ meV, and $\lambda_B=0.12$ meV. These parameter values, slightly different from those given above, were chosen to stabilize the numerical procedure over the entire range of applied biases. The zero field curve has been added in Fig. 5 for the sake of comparison (dashed line). The agreement with the experimental results is quite good. However, there is an extra conduction channel operative for eaF values of 7 meV or more, which breaks the shape of the curve. One possible candidate for this chan-

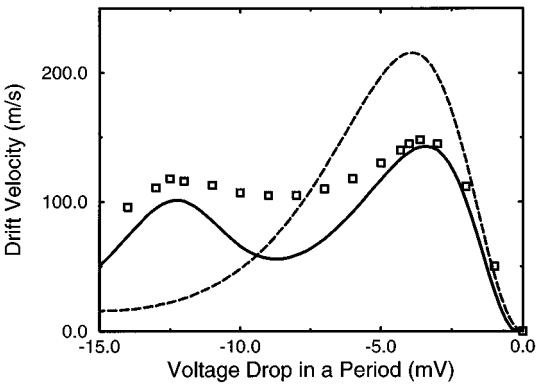

FIG. 5. Drift velocity vs electric field (or applied voltage) for the 11.3-nm–1.7-nm GaAs-AlAs superlattice at 2.4 K. The squares denote the experimental data, the solid line (dashed line) the calculated drift velocity at $B=7$ T ($B=0$ T).

nel is relaxation between Stark levels by emission of multiple acoustic phonons. Also, a dark current may be present. Our calculation includes the hopping current only, thus missing the background contribution due to nonresonant tunneling or due to the dark current. This background, which is expected to increase roughly exponentially with the electric field, would then increase the calculated drift velocity bringing it into better agreement with the experimentally measured values.

The magnetic resonances given by the model and shown in Fig. 5 occur at the expected energies. The model suggests that there is some quenching of the scattering rate due to the magnetic field shifting the maximum drift velocity peak to lower energies for finite B. The same effect would be responsible for reducing the magnitude of this peak compared to the $B=0$ T trace.

Similar time-dependent Schrödinger equation calculations have been performed before for a perfect lattice with no magnetic field.[11,12] The motion was followed over many periods and Wannier-Stark oscillations were readily observed. The dynamical details of our finite size scattering time model with magnetic field are rather complicated. In general as time evolves there is not one, but more than one peak into which the original localized wave function splits. The widths of these peaks, however, decrease with increasing electric field as required from localization considerations. If one starts with a broader initial pulse our results are qualitatively similar, although some boundary effects begin to appear.

IV. SUMMARY AND CONCLUSIONS

We have studied the drift velocity of a photoexcited electron pulse in a GaAs-AlAs superlattice under application of electric and magnetic fields along the growth axis. Besides the peak marking the transition from Ohmic conduction to Wannier-Stark localization, secondary peaks are observed in the negative differential velocity regime, which can be assigned to resonant Landau level tunneling. This interpretation is supported by model calculations of the transport properties of such a system. The comparison between our experimental and calculated drift velocities leads to the conclusion that the transport is mediated by scattering between different Stark, as well as Landau, levels.

ACKNOWLEDGMENTS

This work was supported in part by the Bundesministerium für Bildung und Forschung, Fundación Andes/Vitae/Antorchas, Grant No. 12021-10, FONDECYT Grant No. 1930553, and the Deutsche Akademische Austauschdienst (DAAD). One of us (F.C.) would like to thank the Max-Planck-Institut fur Festkörperforschung in Stuttgart, Germany, for its hospitality while part of this work was being done.

*Present address: Robert Bosch G.m.b.H., FV/FLD, Postfach 10 60 50, D-70049 Stuttgart, Germany.

†On leave at Tokyo Institute of Technology, Research Center for Quantum Effect Electronics, 2-12-1 O-okayama, Meguro-ku, Tokyo 152, Japan.

[1] V.J. Goldman, D.C. Tsui, and J.E. Cunningham, Phys. Rev. B **36**, 7635 (1987).

[2] M.L. Leadbeater, E.S. Alves, L. Eaves, M. Henini, O.H. Hughes, A. Celeste, J.C. Portal, G. Hill, and M.A. Pate, Phys. Rev. B **39**, 3438 (1989).

[3] G.S. Boebinger, A.F.J. Levi, S. Schmitt-Rink, A. Passner, L.N. Pfeiffer, and K.W. West, Phys. Rev. Lett. **65**, 235 (1990).

[4] W. Müller, H.T. Grahn, K. von Klitzing, and K. Ploog, Phys. Rev. B **48**, 11 176 (1993).

[5] H. Schneider, K. von Klitzing, and K. Ploog, Superlatt. Microstruct. **5**, 383 (1990).

[6] H. Schneider, H.T. Grahn, and K. von Klitzing, Surf. Sci. **228**, 362 (1990).

[7] A.A. Ignatov, E.P. Dodin, and V.I. Shashkin, Mod. Phys. Lett. B **5**, 1087 (1991).

[8] R.R. Gerhardts, Phys. Rev. B **48**, 9178 (1993).

[9] G. von Plessen, T. Meier, J. Feldmann, E.O. Göbel, P. Thomas, K.W. Goosen, J.M. Kuo, and R.F. Kopf, Phys. Rev. B **49**, 14 058 (1994).

[10] A. Bouchard and M. Luban, Phys. Rev. B **47**, 6815 (1993).

[11] K. Hacker and G. Obermair, Z. Phys. **234**, 1 (1970).

[12] H.N. Nazareno and J.C. Gallardo, Phys. Status Solidi B **153**, 179 (1989).